



Earth rotation parameters from GPS and BDS: Contributions from MEO and IGSO satellites

Zhenlong Fang ^a, Tianhe Xu ^{a,b}, Wenfeng Nie ^{a,b,*}, Yuguo Yang ^a, Min Li ^a

^a Institute of Space Science, Shandong University, Weihai 264209, China

^b State Key Laboratory of Geo-information Engineering, Xi'an 710054, China

Received 27 April 2022; received in revised form 28 November 2022; accepted 2 December 2022

Abstract

The Earth Rotation Parameters (ERPs) are fundamental transformation parameters to link the celestial reference frame and Earth-fixed reference frame. Global Navigation Satellite System (GNSS) is one of the key technologies to determine the ERPs and BeiDou Navigation Satellite System (BDS) has been constructed completely in 2020. In this study, we present a 2.5-years (01/2020–06/2022) results of the ERPs determination based on the GPS, global BDS (BDS-3), the regional BDS (BDS-2) combined BDS-3 (as BDS solution), Medium Earth Orbit (MEO)-only BDS (BDS-M) and the GPS combined BDS (GC). We take the IERS 14C04 products as reference to evaluate the accuracy of the ERPs estimates. The results of 3-day arc solution show that (1) compared to the estimates based on GPS solution, the GC combined solution achieves an improvement of 1 %, 7 %, 12 %, 3 % and 5 % for X and Y pole coordinates, X and Y pole coordinate rates and LOD, respectively. In detail, for GC solution, the standard deviation (STD) is 62.9 and 57.4 μas for X and Y pole coordinates, 81.3 and 85.7 $\mu\text{as}/\text{d}$ for X and Y pole coordinate rates, 7.8 $\mu\text{s}/\text{d}$ for LOD. (2) the STD of BDS solution is 86.2 μas , 79.9 μas , 118.9 $\mu\text{as}/\text{d}$, 111.5 $\mu\text{as}/\text{d}$, and 11.8 $\mu\text{s}/\text{d}$ for pole coordinates, their rates and LOD, which has an improvement of 10 %, 3 % for pole coordinates, 5 %, 5 % for pole coordinate rates than BDS-3 and BDS-M solutions, respectively. In terms of the STD for LOD, the BDS solution leads to a decrease about 5 % comparing with BDS-3 solution but has little difference with BDS-M solution. (3) From the point view of spectrum analysis, comparing with those from BDS-3 and BDS-M, the spurious signals in the ERPs estimates derived from BDS can be reduced, demonstrating the superior contribution of BDS-2 and IGSO satellites. The GC combination and 3-day arc solution are proved to further mitigate the artificial signals.

© 2022 COSPAR. Published by Elsevier B.V. All rights reserved.

Keywords: BDS-2/3; Polar motion; Length-of-day; BDS hybrid constellation; Spurious signals

1. Introduction

The Earth Rotation Parameters (ERPs) are fundamental geodetic parameters linking the International Celestial Reference Frame (ICRF) and the International Terrestrial Reference Frame (ITRF) (Petit and Luzum, 2010). The ERPs mainly comprise the X and Y pole coordinates (polar motion, PM), their rates, UT1-UTC and length-of-day

(LOD). The Global Navigation Satellite System (GNSS) is one of the most important satellite techniques in calculation of ERPs (Dow et al., 2009; Ferland and Piraszewski, 2009; Mireault et al., 1999; Steigenberger et al., 2006). In contrast to PM, the GNSS technique cannot determine UT1-UTC in an absolute sense because the UT1-UTC is fully correlated with the orbital elements of the satellites, which is the ascending node and the argument of latitude (Rothacher et al., 2001). However, the singularity can be removed by fixing one of the UT1-UTC parameters (e.g., the offset at the beginning of the orbital arc in the case of

* Corresponding author.

E-mail address: wenfengnie@sdu.edu.cn (W. Nie).

the presented processing strategy), to the corresponding value from the reference time series, such as the International Earth Rotation and Reference Systems Service 14C04 (IERS 14C04) products (Zajdel et al., 2020). In this way, the LOD can be estimated. The LOD, which is a negative time derivative of UT1-UTC, is typically estimated based on satellite techniques (Rothacher et al. 1999, 2001; Bizouard et al., 2019). The LOD estimation is sensitive to the perturbations in orbit modeling, especially those related to Keplerian orbit rotation parameters (Rothacher et al., 1999).

Since Global Positioning System (GPS) appeared in 20th century, many researchers have studied ERPs resolution with GPS and other GNSS. From June 1996, the International GNSS Service (IGS) began to generate the final ERPs series based on weighted means of individual IGS analysis center solution instead of the IERS Bulletin B product (Mireault et al., 1999). Steigenberger et al. (2006) reprocessed nine years data of global GPS network from 1994 to 2002 for ERPs estimation, the results of which showed that the mean formal errors for the X and Y polar motion series are 26 and 29 μas . Lutz et al. (2014) also analyzed the ERPs determined by GPS and GLONASS. The results showed that the accuracy of the single GPS solution was 2 ~ 3 times better than that of the GLONASS solution while the GPS/GLONASS combined solution was slightly better than the GPS-only solution. With the development of the Multi-GNSS EXperiment (MGEX; Montenbruck et al., 2017), Zajdel et al. (2020) investigated the PM estimation from the GPS/GLONASS/Galileo solution, which are of similar accuracy to the GPS solution while they have superior quality comparing with those obtained from GLONASS or Galileo. In detail, the scatter of the GPS-based PM residuals with respect to IERS 14C04 are 1.6 and 1.2 times better for the X component as well as 1.5 and 1.3 times better for the Y component, compared to GLONASS and Galileo, respectively. The reason may be that the polar motion estimates are susceptible to deficiencies in the orbit modeling. So far, most researchers mainly focus on ERPs estimation using GPS, GLONASS and Galileo.

In addition to the accuracy of the ERPs, the characteristic of the system-specific bias and spurious effects of ERPs series are well studied. Meindl (2011) showed the differences in ERPs derived from the single GPS and GLONASS system solutions over 3 years. It was found that both solutions for polar motions had visible systematic bias with respect to the IERS 14C04 series. The differences obtained from GLONASS solutions were by a factor of about 1.5 and 2 higher when compared to GPS solutions for X and Y polar motions, respectively. Zajdel et al. (2020) studied the system-specific systematic errors in ERPs derived from GPS, GLONASS and Galileo. The results showed that GPS-based LOD with respect to the IERS 14C04 values had a systematic bias with a mean offset of $-22.4 \mu\text{s/d}$, but Galileo-based solution was almost free of this issue.

As for the system-specific spurious effects, Griffiths and Ray (2013) studied the GPS-based ERPs time series from IGS and detected draconitic errors. Arnold et al. (2015) analyzed different cases of Solar Radiation Parameter (SRP) modeling with different groups of empirical parameters of the Empirical CODE Orbit Model (ECOM) (Beutler et al., 1994). The results indicated that some spurious signals existing in ERPs were attributed to the ECOM, and the proposed new extended ECOM can substantially reduce the spurious signals. A similar conclusion was obtained by Rodriguez-Solano et al. (2014), which showed that the adjustable box-wing model for SRP modeling can significantly mitigate the spurious signals at the draconitic harmonics for the GNSS-based ERPs. Lutz et al. (2016) pointed that the long-arc solution was found to be superior to the 1-day solution for the time series of ERPs. The Root Mean Square Errors (RMSE) of ERPs series were typically reduced between 10 % and 40 %, and the spurious variations in the ERPs as well as the systematic errors in the polar motion coordinates of GLONASS-only solutions were substantially reduced. Scaramuzza et al. (2018) studied the impact of the number of GNSS orbital planes on the geodynamic parameters, including ERPs. The study showed that 3 instead of 6 orbital planes in the GNSS constellation lead to significant spurious signals at 3 cycles per year (cpy) and the combination of different GNSS system, regardless of the orientation of their nodes, can reduce these signals. Dach et al. (2021) analyzed the power spectrum of ERPs midnight discontinuities based on 3-day GNSS solutions, the results of which showed that GPS/GLONASS and GPS/Galileo combined solutions can reduce the magnitude of the spectrum peaks compared to GPS-only solution. However, the noise of GLONASS/Galileo combined solution in the low-frequency range was slightly higher than that of the GPS-only solution. BDS is also an important system for geodetic parameters estimation (Duan et al., 2022; Li et al., 2022; Peng et al., 2022). The impact of solar radiation pressure models on Earth rotation parameters derived from BDS has also been investigated. Duan et al. (2022) and Peng et al. (2022) concluded that a priori box-wing model can improve geodetic parameters in all cases and mitigate a great majority of the spurious signals in the geodetic parameter spectrum.

However, these studies did not analyze the contribution of BDS to the GPS-only solution, which is used by IGS and IERS products. Since BDS has hybrid constellation structure of Geostationary Earth Orbit (GEO), Inclined Geostationary Orbit (IGSO) as well as Medium Earth Orbit (MEO) satellites and the hybrid constellation of BDS satellites have diverse orbit revolution periods, this may give us a new insight on the characteristic of the ERPs.

Therefore, we present the results to investigate the influence of constellation configuration on BDS solution and the contribution of BDS in the combination of GPS/BDS solution using 2.5-years data from January/2020 to June/2022. We first introduce the research background

and current situation of the ERPs estimation. In the next sections, we briefly describe the method used in the ERPs determination, and then the description is focused on the experiments and results obtained from 2.5 years of observation data. As stressed by Ray et al (2017), Geocenter Coordinates (GCC) and PM should be analyzed simultaneously as GCC and PM errors are correlated in particular for a sub-optimal GNSS distribution. Thereafter, analyses of the estimated ERPs and orbit as well as GCC are presented, followed by conclusions in the last section.

2. Methodology

All computations made in this study are performed with the Bernese GNSS software (Dach et al., 2015), which is modified to support BDS data processing by our own research group. The details about the methodology adopted are summarized in Table 1. Considering the B1 and B3 signals are common for BDS-2 and BDS-3 systems, we use the combination of B1 and B3 signals for data processing in this study. Because the information of satellite dimensions and optical properties is limited, empirical models are widely used for SRP modeling. Despite ECOM is well adapted to GPS, the model has some deficiencies in data processing for GLONASS, Galileo, BDS and QZSS (Prange et al., 2017). Arnold et al. (2015) updated ECOM

to ECOM2, using Δu as the angular argument instead of the argument of latitude u , and adding second- and fourth-order harmonic terms to D component (pointing from the satellite to the Sun):

$$\begin{aligned} a_D &= D_0 + D_{C2} \cdot \cos 2\Delta u + D_{S2} \cdot \sin 2\Delta u + D_{C4} \cdot \cos 4\Delta u \\ &\quad + D_{S4} \cdot \sin 4\Delta u \\ a_Y &= Y_0 \\ a_B &= B_0 + B_C \cdot \cos \Delta u + B_S \cdot \sin \Delta u \end{aligned} \quad (1)$$

Where $\Delta u = u - u_S$ represents the angular argument, with u_S being the argument of latitude of the Sun projected on the orbital plane.

The latest BDS-3 MEO satellites exhibit a rectangular shape with a ratio of about 2:1 for the main body axes (MGEX, 2020), which are similar to Galileo satellites. Prange et al. (2017) showed that ECOM2 performed well for the Galileo satellite with a stretched body. In this study, we use the empirical ECOM2 model with 7 parameters (3 constant accelerations in DYB directions, sine and cosine once-per-revolution terms in B, and sine and cosine twice-per-revolution terms in D) for the SRP modeling (Prange et al., 2020). Since the high correlations of length of day (LOD) with the periodic dynamic parameters in the D and Y directions in ECOM2 model, we freely esti-

Table 1
Description of the processing strategy.

Processing feature	Adopted processing strategy
GNSS considered	BDS-2/3; IGSO/MEO; GPS
Time span	2.5 years: 01/2020–06/2022
Number of stations	~ 100 stations
Processing scheme	Double-difference network processing with ionospheric-free linear combination observations
Signals	B1 + B3 for BDS; L1 + L2 for GPS
Observation sampling	180 s
Arc length	24 h and 72 h
Elevation cut-off angle	3 degrees
Gravity field model	EGM 2008, 12 × 12 degree (Pavlis et al., 2012)
N-body gravitation	JPL DE405 ephemeris (Standish, 1998)
A priori reference frame	IGS14 (Rebischung et al., 2016a)
Phase center offsets (PCO) and phase center variations (PCV)	IGS14.ATX (https://files.igs.org/pub/station/general/igs14.atx ; Rebischung et al., 2016b), BDS satellites PCV: ignored
Loading corrections	Ocean loading corrections: FES2004 (Lyard et al., 2006)
Earth rotation parameters	A priori ERPs: IERS 14C04 (Bizouard et al., 2019), only UT1-UTC constrains to 0.0001 mas; Polar motion, their rates and LOD are estimated
Datum definition	Minimum constraint with no-net-translation and no-net-rotation conditions with respect to IGS14 reference frame
Station coordinate	Each station coordinate is estimated with no-net-translation and no-net-rotation
SRP model	ECOM2 7 parameters (Arnold et al., 2015)
Pseudo-stochastic pulses (sigma)	D0, D2S, D2C, Y0, B0, B1C, B1S (7 parameters) are estimated Each midnight epochs in the along-track (10^{-5} m/s), cross-track (10^{-8} m/s), radial (10^{-6} m/s), after Dach et al. (2009)
Troposphere delay	GMF with 2-h resolution of station-specific troposphere parameters (Boehm et al., 2006), gradients with 24-h resolution (Chen and Herring, 1997); Zenith wet delay and gradient parameters are parametrized as piecewise constraints
Solid Earth tides, pole tides	IERS Conventions 2010 (Petit and Luzum, 2010)
Orbit parameters	Satellite positions and velocity (X, Y, Z, Vx, Vy, Vz) are estimated
Geocenter coordinates	Estimated without constraint

mate all parameters but constrain the parameters in the D and Y directions with a priori sigma of 10^{-12} m/s² (Dach et al., 2015).

The tracking data from the MGEX performed by the IGS are used to estimate ERPs for 1-day and 3-day arc. The data processing progress is implemented with batch mode by moving time window. The 3-day arc solution is based on the stacked 1-day normal equation systems (NEQs) of three consecutive days separated by 1-day intervals, which means that the middle day of one solution overlaps the first day of the subsequent solution. In 1-day arc solution, the ERPs are parametrized by the offset and rate at noon for each day independently, as in line with the current IGS requirements (Kouba and Mireault, 1998). For the 3-day arc solution, the ERPs are represented by 3-day offsets and rates at noon for each ERPs component. Additionally, the equal weight scheme is adopted for BDS-2, BDS-3 and GPS observations in GPS and BDS combined solution and the specific-system solution. In total, the computation of all the 5 solutions which include GPS, BDS-3, BDS-M (MEO-only BDS), BDS (BDS-2 combined BDS-3) and GC (the combined GPS and BDS) are based on the same NEQs from GC solution. In this study, all the solutions share part of parameters such as troposphere and station coordinate but estimate orbit, GCC and ERPs individually. By using the same NEQs as a basis for each solution, we can ensure the consistent and terrestrial reference frame is the same for all solutions in the parameter estimation (Scaramuzza et al., 2018).

Fig. 1 shows the global homogeneous distribution of about 100 stations. **Fig. 2** shows the number of stations tracking BDS satellites at the different stages from January/2020 to June/2022.

For BDS, we only consider IGSO and MEO constellation because GEO satellites is with little geometry change, which makes it difficult to separate clock and atmospheric delays from satellite positions. Thus, the obvious orbital errors of GEO satellites would result in diurnal ERPs changes. In **Fig. 2**, the satellites of C06, C07, C08, C09, C10, C13, C16 are belonging to the IGSO of BDS-2 while those of C38, C39, C40 are IGSO satellites belonging to

BDS-3. In our data processing, we use about 10 BDS-2 satellites. It is noted that the **IGSO constellation is a regional system**, so the number of its observing stations is smaller than MEO constellation. For BDS-3, only MEO satellites from C19 to C37 are considered in 2020 when most of receivers cannot track more BDS-3 satellites. From 2021 to 2022, about 27 BDS-3 satellites are used in our data processing. **Fig. 3** shows the total number of BDS satellites and stations in the data processing. It can be seen that there is an obvious increasement of the number of BDS satellites in January/2021.

3. Results

In this section, the analysis of ERPs derived from GPS and BDS is presented. The estimates of the X and Y pole motion, their rates and LOD are compared to the reference values of IERS 14C04 (Bizouard et al., 2019). The **IERS 14C04** series is provided by the IERS servers at both noon and midnight epochs (https://hpiers.obspm.fr/iers/eop/eopc04/eopc04.dX_dY.12h.84-now, https://hpiers.obspm.fr/iers/eop/eopc04/eopc04_IAU2000.62-now). The IERS series is a multi-technique solution at the NEQs level, combining the Very Long Baseline Interferometry (VLBI), Satellite Laser Ranging (SLR), Doppler Orbitography and Radiopositioning Integrated by Satellite (DORIS) and GNSS data. The combined solution benefits from the advantages of various geodetic techniques, while most of their weaknesses are averted. We should be aware that IERS 14C04 series is smoothed, losing most of the real PM signal, especially at the 1–2 days window and affecting signals with periods up to 3 days (Zajdel et al., 2020). Bizouard et al. (2019) assessed the general consistency of the GNSS-based IGS results within the IERS 14C04 combination for the period 2010–2015, which reached an impressive level of 30 μ as and 10 μ s/d for PM and LOD, respectively. In the last part of this section, we discuss the ERPs overlaps of 3-day arc as the internal quality indicator.

3.1. Evaluation of orbit results

Since ERPs are used to link the ICRF and the ITRF and the satellite orbits are usually determined in an inertial system, ERPs are always estimated with satellite orbits at the same time. Therefore, we analyze the quality of orbit by comparing with ESA Multi-GNSS products (<http://navigation-office.esa.int/products/gnss-products/>; Mayer et al., 2019) for 1-day and 3-day solutions and by using overlaps between consecutive arcs of 3-day arc solution in the inertial frame.

Table 2 shows the mean value of the 1D RMS for orbit with respect to ESA Multi-GNSS products. The change of the orbital arc length from 1 to 3 days results in the improvement of the consistency with ESA Multi-GNSS products. The most obvious one is BDS-3 in GC solution. The 1-day arc mean RMS is 4.0 cm and the value in 3-day

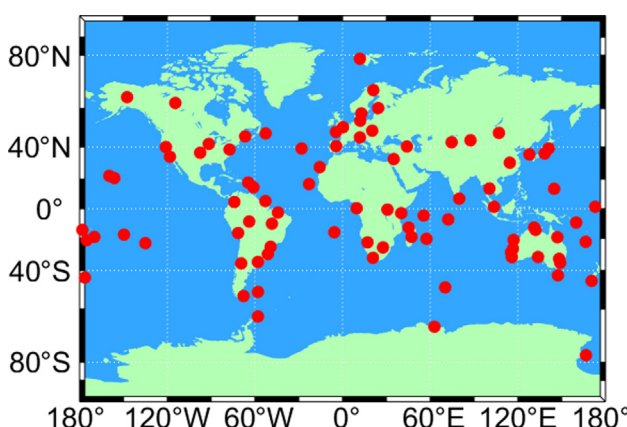


Fig. 1. Distribution of about 100 MGEX stations used in this study.

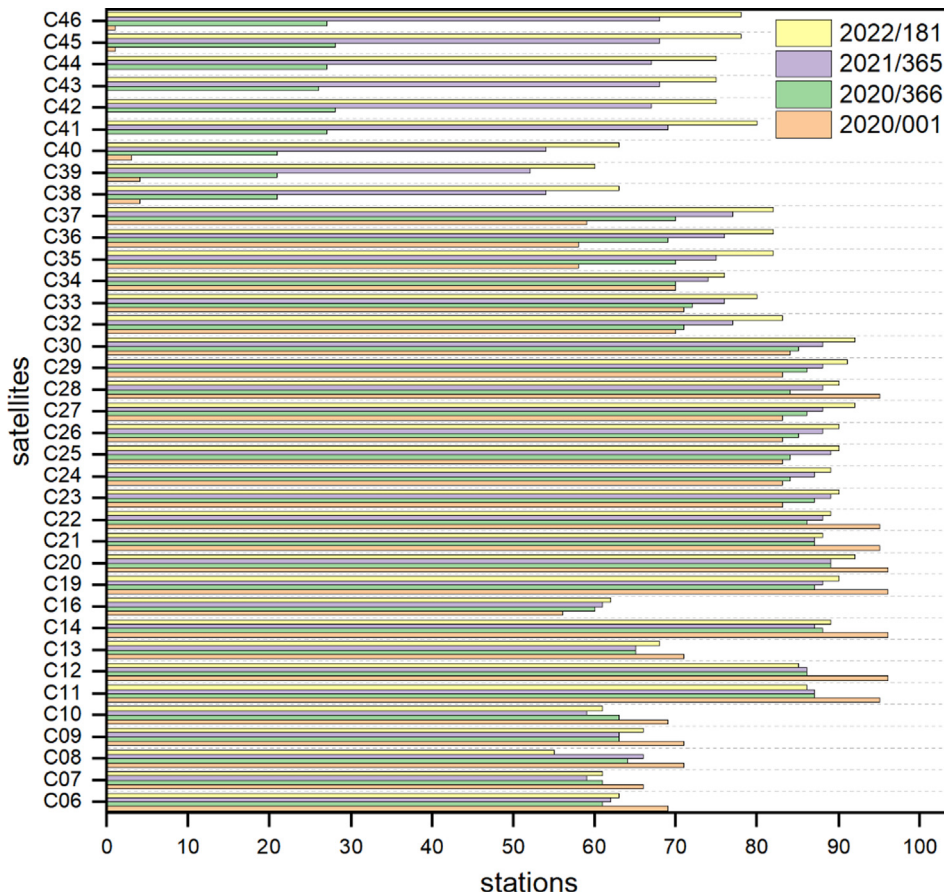


Fig. 2. The number of observing stations for each BDS satellite in our data processing (the day of year 001 and 366 in 2020, 365 in 2021 and 181 in 2022).

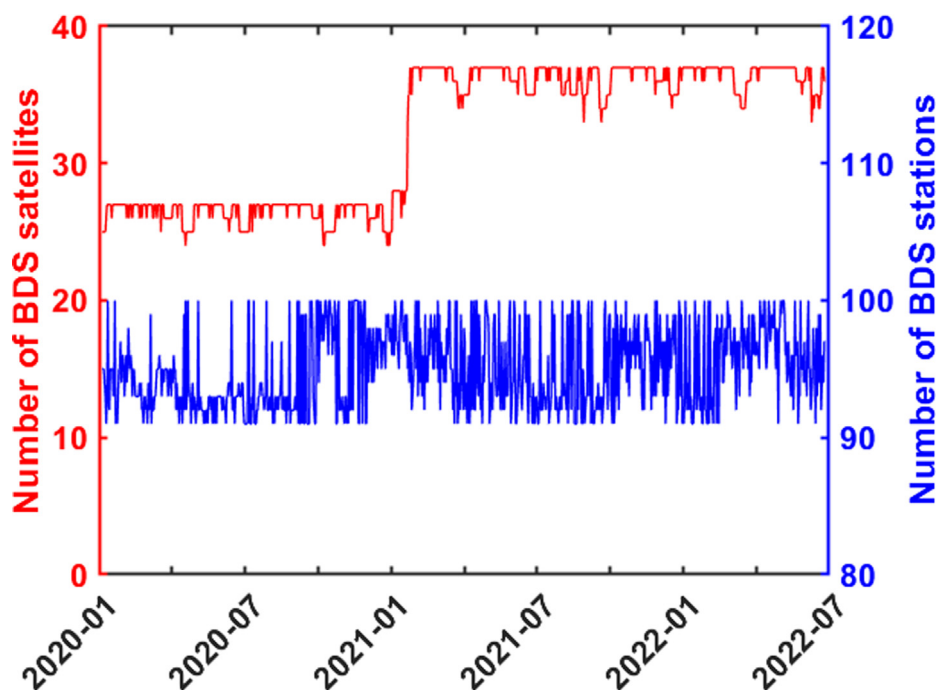


Fig. 3. Time series of the total number of BDS satellites and stations in the data processing.

Table 2

Mean value of the orbit RMS in 1D direction with respect to ESA Multi-GNSS products in the inertial frame (unit: cm).

System	Solution	1-day arc	3-day arc	Improvement
BDS-2	BDS-M	3.8	3.2	15.8 %
	BDS	6.9	6.2	10.1 %
	GC	6.1	5.9	3.3 %
BDS-3	BDS-3	4.2	3.8	9.5 %
	BDS-M	3.6	3.2	11.1 %
	BDS	4.1	3.6	12.2 %
GPS	GC	4.0	3.2	20.0 %
	GPS	1.9	1.7	10.5 %
	GC	1.8	1.7	5.6 %

solution reduce to 3.2 cm, which achieves an improvement of 20 %. In the MEO-only solution, the mean values of RMS for BDS-2 and BDS-3 are about 3.2 cm. However, when including IGSO satellites, the mean RMS increases to about 6.2 cm and 3.6 cm, which may attribute to the worse observation geometry for IGSO.

The middle day of the 3-day arc compared with the consecutive day can be treated as the overlapping arc. We summarize the mean RMS of orbit overlaps for 3-day arc solutions in Table 3. The mean values in each solution for BDS-2 and BDS-3 are between 1.5 cm and 2 cm while those for GPS are about 1 cm. The GC combined solution

Table 3

Mean value of 1D RMS for the orbit overlaps between consecutive arcs in inertial frame (unit: cm).

Solution	System		
	BDS-2	BDS-3	GPS
BDS-3	–	1.9	–
BDS-M	1.6	1.6	–
BDS	1.9	1.8	–
GPS	–	–	1.1
GC	1.7	1.6	1.0

Table 4

Mean formal solution errors for the respective solutions.

(a)

	X (μas)		Y (μas)		1-day	3-day
	1-day	3-day	1-day	3-day		
BDS-3	34.6	17.6	36.7	19.3		
BDS-M	28.8	14.5	30.3	15.5		
BDS	22.1	12.6	24.9	13.9		
GPS	16.6	9.0	17.6	9.3		
GC	14.9	8.7	17.0	9.2		

(b)

	Xrt (μas/d)		Yrt (μas/d)		LOD (μas/d)	
	1-day	3-day	1-day	3-day	1-day	3-day
BDS-3	72.4	22.8	85.0	22.3	4.6	1.0
BDS-M	66.6	21.4	78.9	20.4	4.2	1.0
BDS	55.2	16.3	64.2	17.4	3.6	0.8
GPS	31.8	12.2	38.4	12.2	1.9	0.6
GC	30.3	11.8	34.7	12.1	1.8	0.5

have better performance than system-specific solutions. With the inclusion of IGSO satellites, the mean RMS for BDS-2 and BDS-3 is worse than BDS-MEO only solution.

3.2. Formal errors of Earth rotation parameters

The formal errors of the ERPs estimate for respective solutions are summarized in Table 4. The change of the orbital arc length from 1 to 3 days results in smaller mean formal errors. The mean formal errors are reduced from 1.7 to 2 times for PM, from 2.5 to 4 times for PM rates and from 3.5 to 5 times for LOD, when using 3-day arc compared to 1-day arc. Especially for BDS-3, BDS-M and BDS cases, the mean formal errors of 3-day arc solutions are even about 3.5 times and 4.4 times smaller than 1-day arc solutions. Since more observations are used, the reduction of formal errors should be attributed to the extension of orbital arc length, strengthening the continuity of orbits and ERPs over the orbital arc. In this way, the correlations between parameters get reduced in the 3-day solutions (Lutz et al., 2016). With the inclusion of BDS-2 satellites, the BDS solution has an improvement of about 25 % comparing with BDS-3. To investigate the contribution of IGSO satellites, the difference of formal errors for BDS solution with BDS-M solution is also presented in Table 4 and the results show that BDS solution has smaller mean values by 20 % than BDS-M solution. Compared with GPS solution, the GC combination solution leads to a decrease of about 5 % in mean formal errors.

Fig. 4 and Fig. 5 show the time series and the spectral analysis of the formal errors from the particular solutions obtained in the 1-day and 3-day arc cases. From the time series, we can see that the range of formal errors variation is reduced from 80 to 40 μas for pole coordinates as well as from 8 to 4 μas/d for LOD, and the time series become more stable since July/2021 for BDS-3, BDS-M and BDS solutions. The reason may be that more and more stations support observing more BDS-3 satellites (from Fig. 2 and Fig. 3). The formal errors from 1-day arc solutions for LOD always vary in time significantly, while the variances are reduced almost to zero in 3-day arc solution. These obvious variations most likely originate from the strong correlation between LOD and the sun elevation above orbital planes (Peng et al., 2022; Zajdel et al., 2020). From the amplitude spectra of the formal errors, the most obvious signals for LOD are at the frequency of 2, 4, 6 and 8 cpy for all BDS satellites. However, the GC combination as well as the extension of orbital arc can mitigate most of the periodic signals.

3.3. Polar motion

We present the mean offset and STD of the PM with respect to the IERS 14C04 in Table 5. The mean offset for 3-day arc solution equal 66.9, 51.0, 23.7, 12.1, 10.1 μas for X coordinates and 28, 19.7, 41.6, 7.2, 4.2 μas for the Y coordinate, for BDS-3, BDS-M, BDS, GPS and

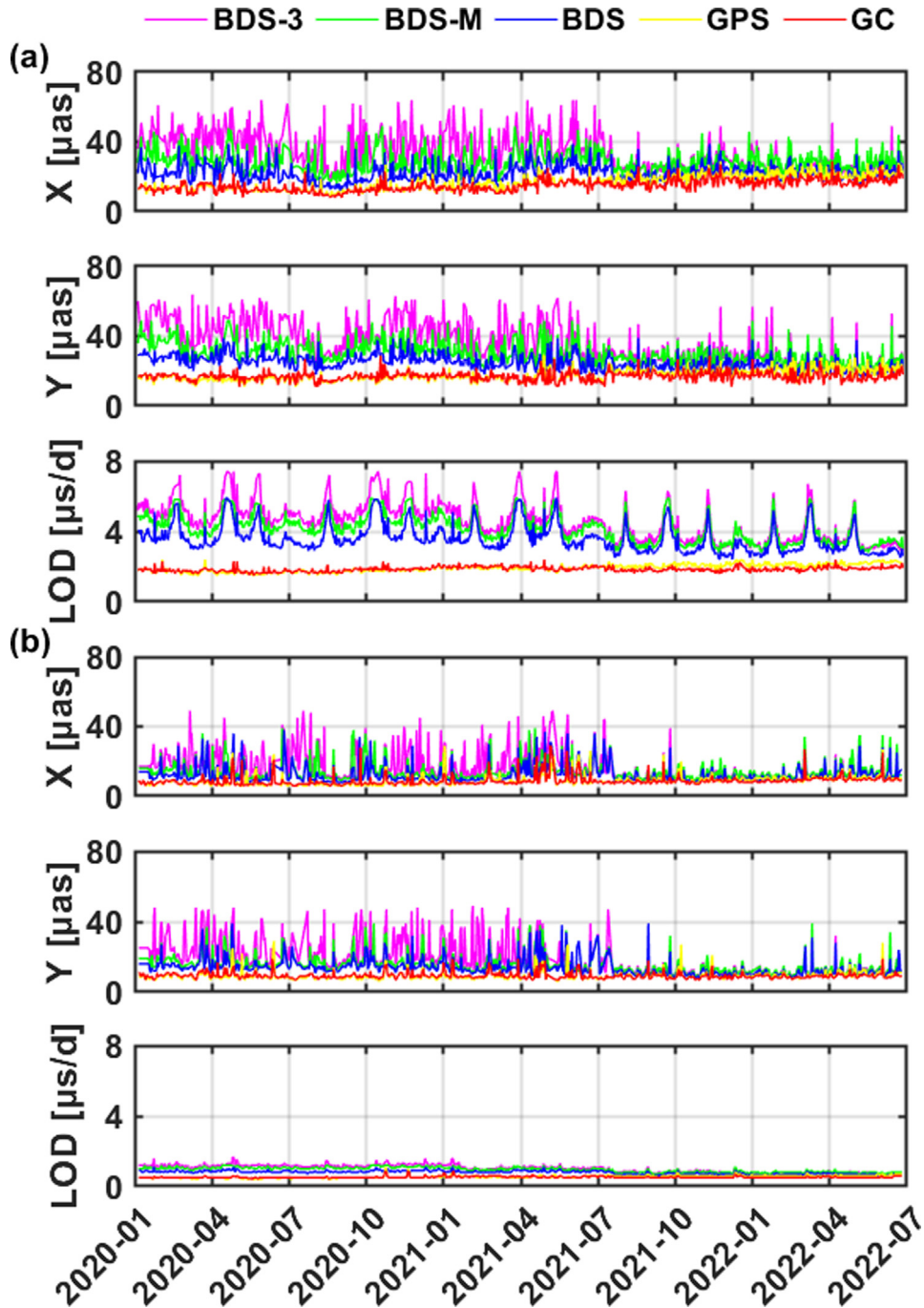


Fig. 4. Time series of X_p , Y_p and LOD formal errors from the respective (a) 1-day arc solution and (b) corresponding 3-day arc solution.

GC, respectively. With the inclusion of BDS, the mean offsets of GC combination solution are about 1.5 times smaller than GPS solution. The extension of orbital arc length has little effect on the mean offset of BDS-3, BDS-M and BDS solutions. In addition, the mean offsets of BDS-3, BDS-M and BDS solutions are 2 times larger than GPS and GC solutions. These obvious mean offsets in PM for BDS-2 and BDS-3 satellites may original from the lack of accurate phase center offsets (Peng et al., 2022; Zajdel et al., 2020) and the other possible reason is that IERS

14C04 series is taken as a reference which is dominated by GPS (Bizouard et al., 2019).

In terms of STD in 3-day arc solution, GPS and GC solution results are scattered having a STD of approximately 60 μas for pole coordinates. In contrast, the STD for BDS-3, BDS-M and BDS solutions is about 80–95 μas . With the inclusion of BDS-2, the STD for BDS has an improvement of 10 % comparing with BDS-3. Comparing with BDS-M solution, the inclusion of IGSO can lead to a decrease of about 3 % in STD for BDS. The GC com-

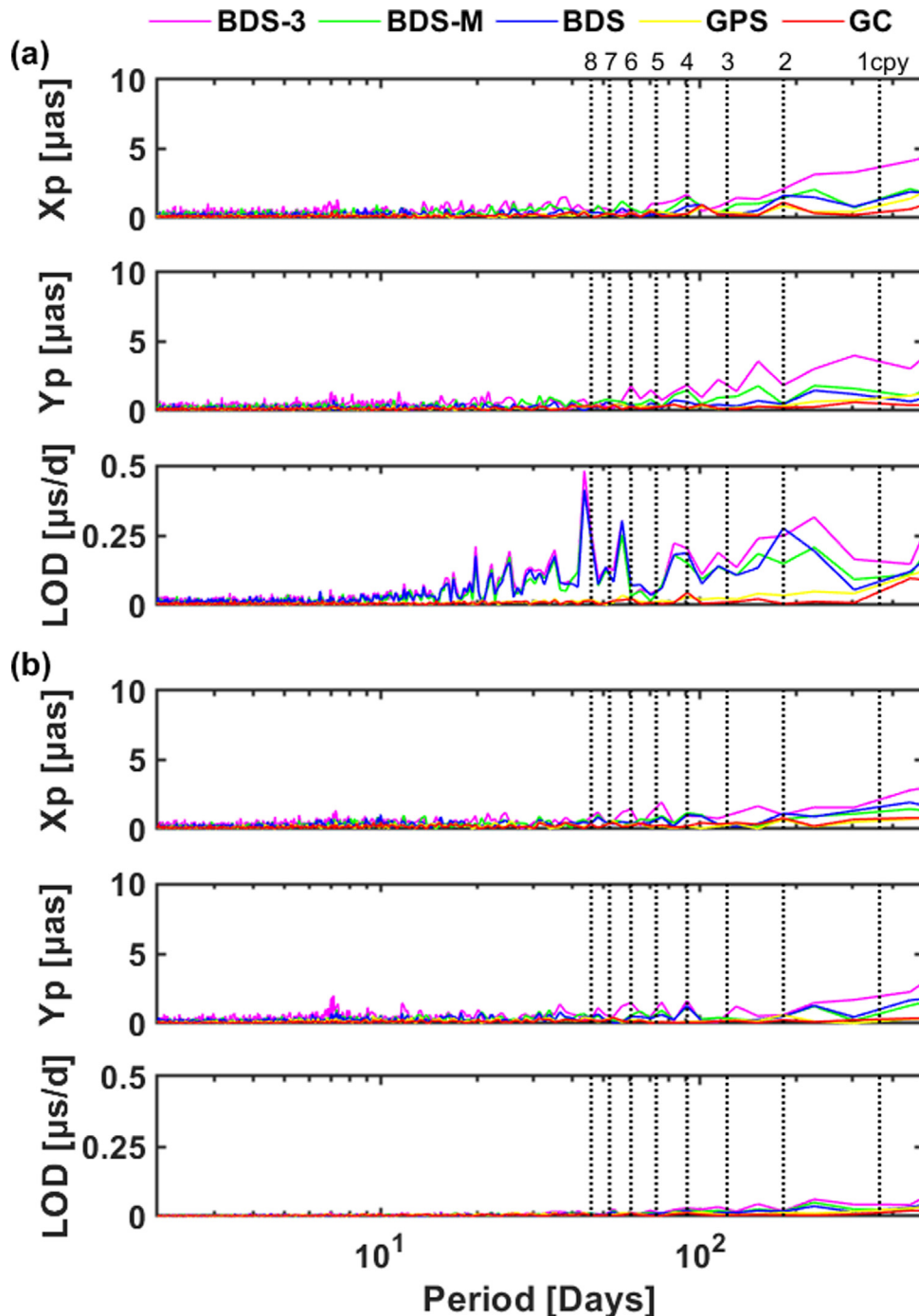


Fig. 5. Amplitude spectra of X_p , Y_p and LOD formal errors from the respective (a) 1-day arc solution and (b) corresponding 3-day arc solution. The vertical gray lines denote the harmonics of a draconitic year.

bination solution achieves an improvement of 2 % than GPS solution. The STD of 3-day arc solutions is about 1.4 times better than 1-day arc solutions for X and Y coordinates.

From Fig. 6, it can be seen that the PM residuals of BDS solution are smaller and more stable than those of BDS-3 and BDS-M solutions, and the range of their variation is about 300 μas . The 3-day arc solution has more stable time series and the range of variation decreases about half of the 1-day arc solution. Since July/2021, the residual time series

are more stable than before, because of the increase of BDS-3 observations.

Fig. 7 illustrates the spectral analysis of the X and Y pole coordinate differences with respect to IERS 14C04. The X pole coordinate is more sensitive to spurious signals than the Y pole coordinate. The most significant signals of X pole coordinate occur in 3 cpy with an amplitude up to 80 μas for BDS-3, BDS-M, BDS and GC solutions. These strong signals at the 3rd harmonics of the draconitic year in X pole coordinate may attribute to the 3-plane constella-

Table 5
Statistics of the pole coordinate differences with respect to IERS 14C04.

	1-Day arc		3-Day arc	
	Mean	STD	Mean	STD
X (μas)				
BDS-3	46.0	148.2	66.9	94.7
BDS-M	30.4	125.1	51.0	87.9
BDS	4.1	121.4	23.7	86.2
GPS	-4.0	82.7	12.1	63.3
GC	-1.9	78.5	10.1	62.9
Y (μas)				
BDS-3	21.1	132.3	28.0	94.0
BDS-M	19.4	122.1	19.7	84.0
BDS	52.1	119.0	41.6	79.9
GPS	54.9	82.0	7.2	61.7
GC	41.8	81.9	4.2	57.4

tion such as Galileo, GLONASS and BDS (Peng et al., 2022; Zajdel et al., 2020). The amplitude of 3 cpy signal for BDS solution is smaller than BDS-3 and BDS-M,

which means the inclusion of BDS-2 and BDS-M can reduce the impact of spurious signals. The GC combination solution and 3-day arc solution can reduce the 3 cpy signals but cannot mitigate them completely. In addition, there is a clear signal close to 7 cpy (52 days) with an amplitude about 25 μas for BDS-3, BDS-M and BDS, which also affect other 3-plane constellations and may be caused by the deficiencies of orbital modeling (Peng et al., 2022; Zajdel et al., 2020). Moreover, obvious spurious signals occur in the period of 7.0 days with an amplitude of 25 μas for all BDS solutions, which may originate from the resonance between Earth rotation and satellites revolution because the orbit repeat period of BDS-3 MEO satellites is about 7 days (Peng et al., 2022).

3.4. Polar motion rates

The mean offset, STD of the estimated pole coordinate rate residuals with respect to the IERS 14C04 are summa-

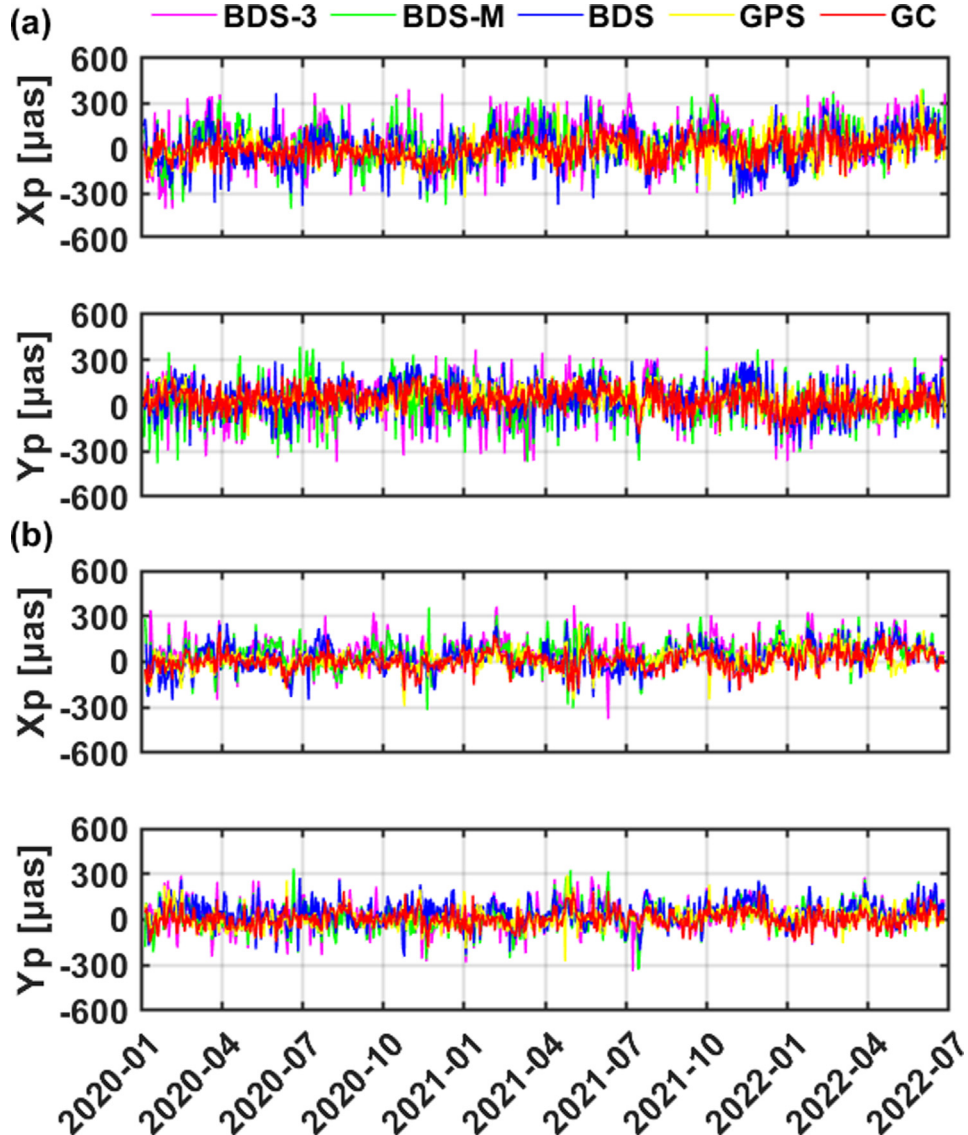


Fig. 6. Time series of PM residuals with respect to IERS 14C04 in X component and Y component from (a) 1-day arc solution and (b) 3-day arc solution.

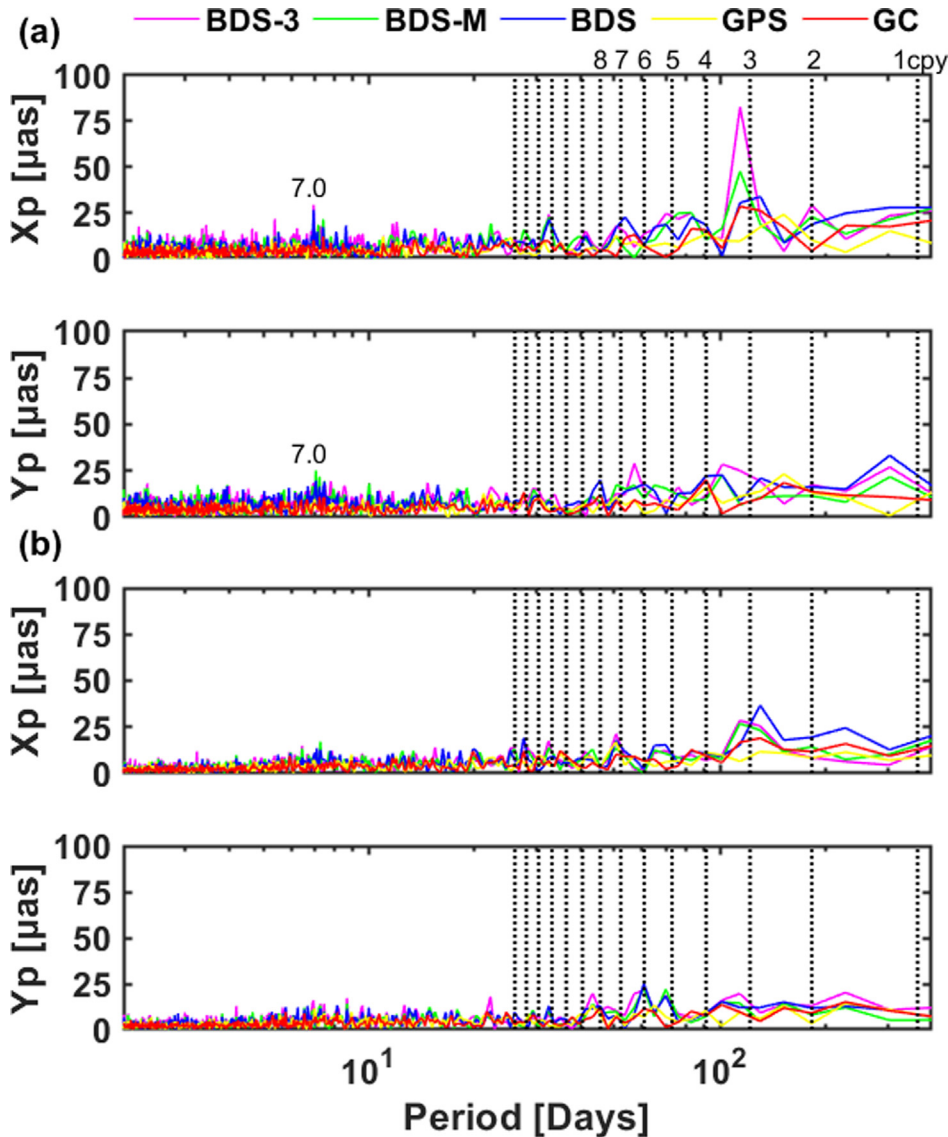


Fig. 7. Amplitude spectra of the estimated pole coordinates with respect to the IERS 14C04 series in X and Y components from (a) 1-day arc solution and (b) 3-day arc solution. The vertical gray lines denote the harmonics of a draconitic year.

Table 6
Statistics of the polar motion rate differences with respect to IERS 14C04.

	1-Day arc		3-Day arc	
	Mean	STD	Mean	STD
<i>Xrt</i> (μas/d)				
BDS-3	88.0	268.7	-19.8	126.7
BDS-M	78.1	244.8	-19.0	124.9
BDS	93.0	229.7	-15.5	118.9
GPS	91.2	153.4	-12.0	92.9
GC	44.5	131.9	-12.1	81.3
<i>Yrt</i> (μas/d)				
BDS-3	-6.5	399.5	6.7	117.7
BDS-M	3.0	330.4	7.5	112.6
BDS	0.3	317.9	4.5	111.5
GPS	-8.5	181.4	3.2	88.2
GC	-10.0	147.3	1.5	85.7

rized in Table 6. In terms of mean offset, the values of 3-day arc solutions are approximately 16 μas/d for X component and 4 μas/d for Y component. When switching from 1-day arc to 3-day arc, the mean offsets for X rate is even 4 times better. In terms of STD, the values of 1-day arc solutions in the case of BDS-3, BDS-M and BDS are larger than 200 μas/d for Xrt and 300 μas/d for Yrt. However, the extension of orbital arc from 1 to 3 leads to 2–3.5 times smaller for BDS-3, BDS-M, BDS solutions and 1.5–2 times smaller for GC and GPS solutions, which is consistent with the conclusion from Lutz, et al. (2016). As a result, the STD of 3-day arc solutions are 126.7, 124.9, 118.9, 92.9, 81.3 μas/d for Xrt and 117.7, 112.6, 111.5, 88.2, 85.7 μas/d for Yrt, for BDS-3, BDS-M, BDS, GPS and GC, respectively. Moreover, the BDS solution gets an improve-

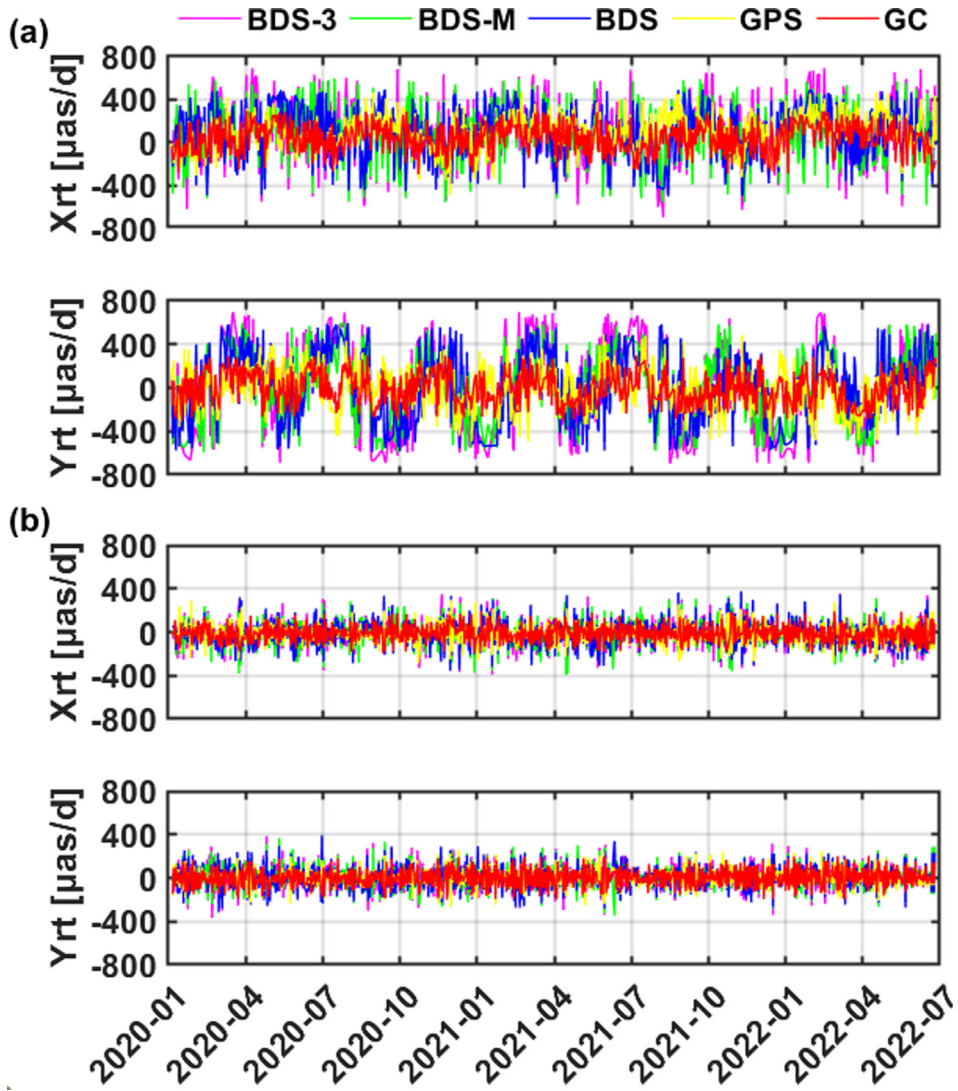


Fig. 8. Time series of polar motion rates residuals with respect to IERS 14C04 in X and Y components from (a) 1-day arc solution and (b) 3-day arc solution.

ment of about 5 % comparing with BDS-3 and BDS-M solutions. The GC combination solution achieves an improvement of 12 % in X component and 3 % in Y component comparing with GPS solution for pole coordinate rates.

Fig. 8 shows the time series of X and Y polar motion rates residuals with respect to IERS 14C04. The results illustrate that the time series of polar motion rates vary significantly in 1-day arc solution and the range of variation for BDS solution is smaller than BDS-2 and BDS-M. Besides, the variation of the polar motion rates for GC combination solution is smaller than that for GPS. When the orbital arc changed from 1 to 3, the time series become stable for all solutions.

Fig. 9 illustrates the spectral analysis of the PM rates. The similar artificial signals in amplitude spectra are also visible in **Fig. 7**. In a circular polar motion of angular velocity ω , we may expect that $\dot{\gamma} = \omega x$ (ω is angular velocity of the Earth rotation). Thus, the Y component of pole

coordinate rate is more vulnerable to spurious signals than X component. The strong signal at 3 cpy with the amplitude about 400 μas/d is evident for BDS-3 and the BDS solution has smaller signal than BDS-3 as well as BDS-M solutions. The pronounced peaks appear at the period of 7 days in X component of pole coordinate rate, which is similar to the pole coordinate. This may be introduced by the resonance between Earth rotation and satellite revolution. Fortunately, these spurious signals including the draconitic year signal are almost completely mitigated when the orbital arc length extends from 1 to 3 days.

3.5. Length-of-day

Since the GNSS satellites are not able to determine the UT1-UTC directly, we can estimate the length of day and fix the first epoch of UT1-UTC to IERS 14C04 products to calculate UT1-UTC.

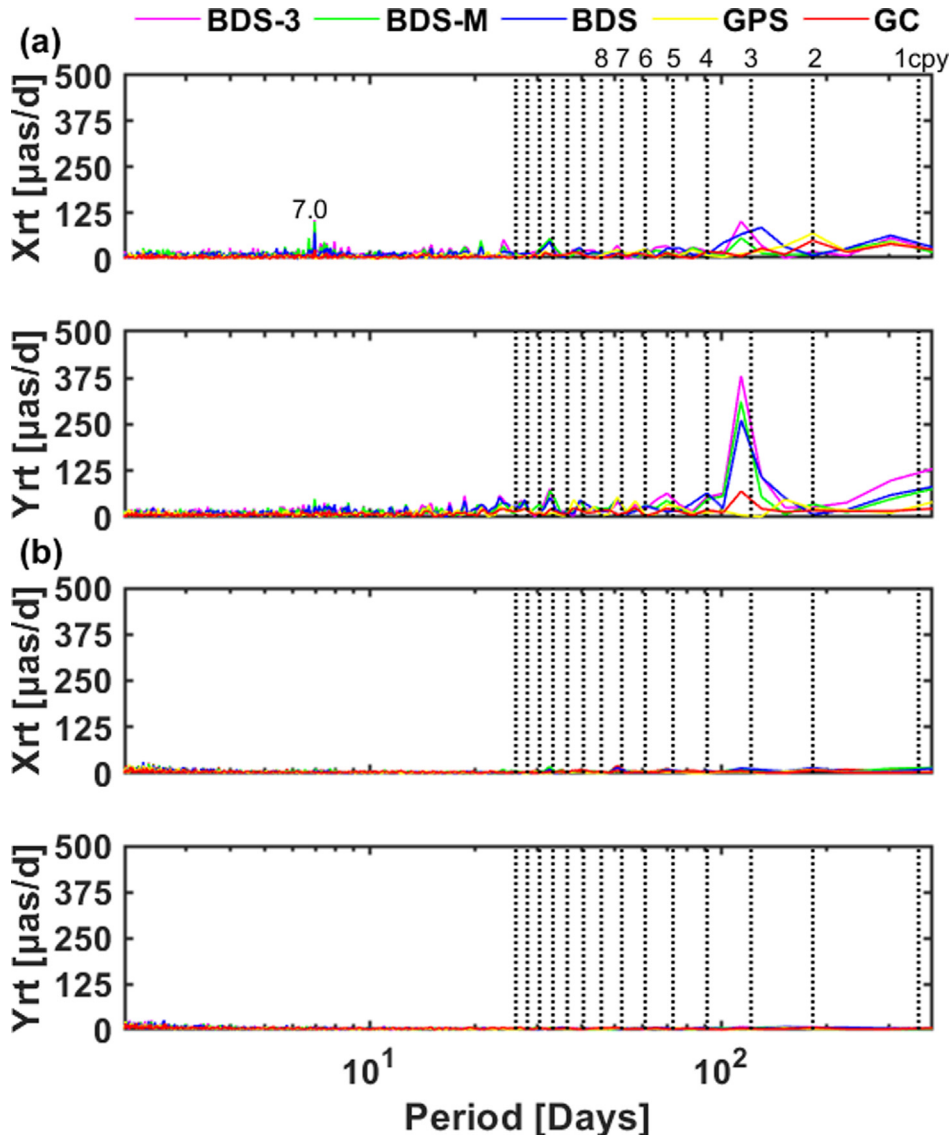


Fig. 9. Amplitude spectra of the polar motion rate residuals with respect to IERS 14C04 in X and Y components from (a) 1-day arc solution and (b) 3-day arc solution. The vertical gray lines denote the harmonics of a draconitic year.

Table 7
Statistics of the LOD differences with respect to IERS 14C04.

	1-Day arc		3-Day arc	
	Mean	STD	Mean	STD
LOD ($\mu\text{s}/\text{d}$)				
BDS-3	1.1	16.5	-3.2	12.5
BDS-M	0.7	15.7	-4.5	11.9
BDS	2.1	15.5	-4.0	11.8
GPS	-11.4	8.4	-7.6	8.2
GC	-7.6	8.6	-6.4	7.8

We summarize the mean offset and STD of the estimated LOD residuals with respect to the IERS 14C04 in Table 7. The mean offsets of the LOD for GPS are visible, which are 2–5 times larger than BDS-based LOD. This may be related to the strength of resonance between the Earth's rotation and the orbital period which is 2:1 for GPS and

17:9 for BDS (Peng et al., 2022). With the inclusion of BDS, the GC combination can reduce the mean offset by 16 % comparing to GPS solution. In addition, the extension of arc length also has positive effects on this term, which can get an improvement of 33 %. Fig. 10 and Table 7 show that the change of orbital length from 1 to 3-day arc makes the stability with a visible improvement and the range of time series variation decreased from 50 to 25 $\mu\text{s}/\text{d}$ for BDS-3, BDS-M and BDS. The STD of 3-day arc solution is 1.3 times smaller than 1-day arc solution for BDS-3, BDS-M and BDS. The 3-day arc solution has an improvement of 5 % comparing to 1-day arc solution for GC and GPS solutions. The STD values of 3-day arc solution are about 12.5, 11.9, 11.8, 8.2 and 7.8 $\mu\text{s}/\text{d}$ for BDS-3, BDS-M, BDS, GPS and GC, respectively. The inclusion of IGSO satellites in BDS solution has little effects on LOD determination comparing to BDS-M results, which may because the IGSO satellites are regional

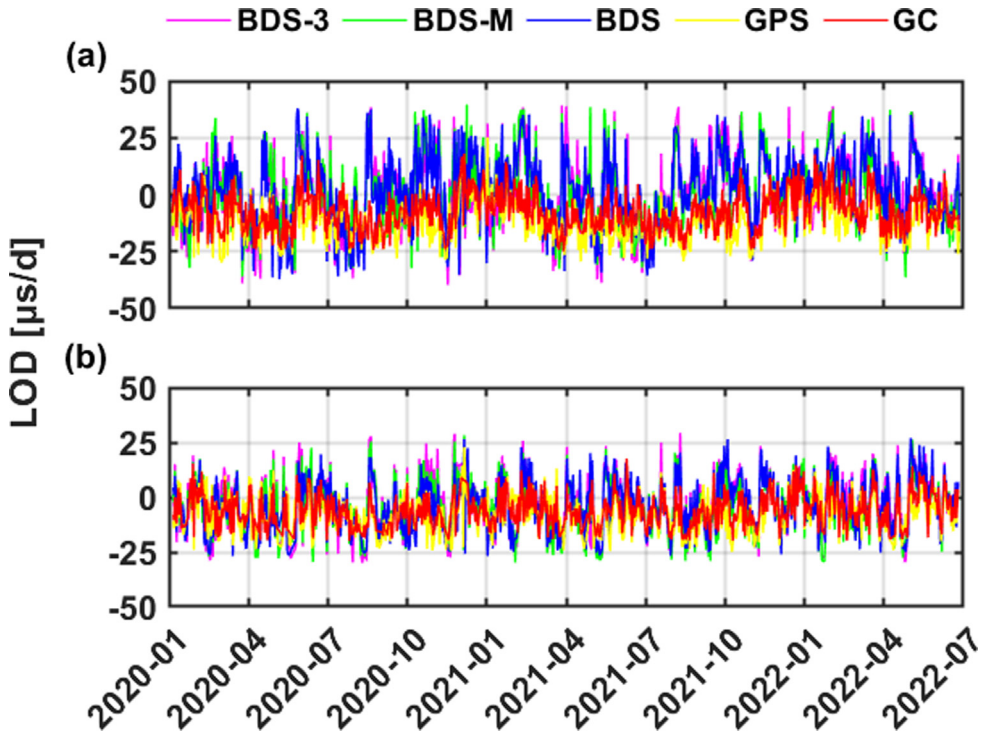


Fig. 10. Time series of LOD residuals with respect to IERS 14C04 from 1-day arc solution (top) and 3-day arc solution (bottom).

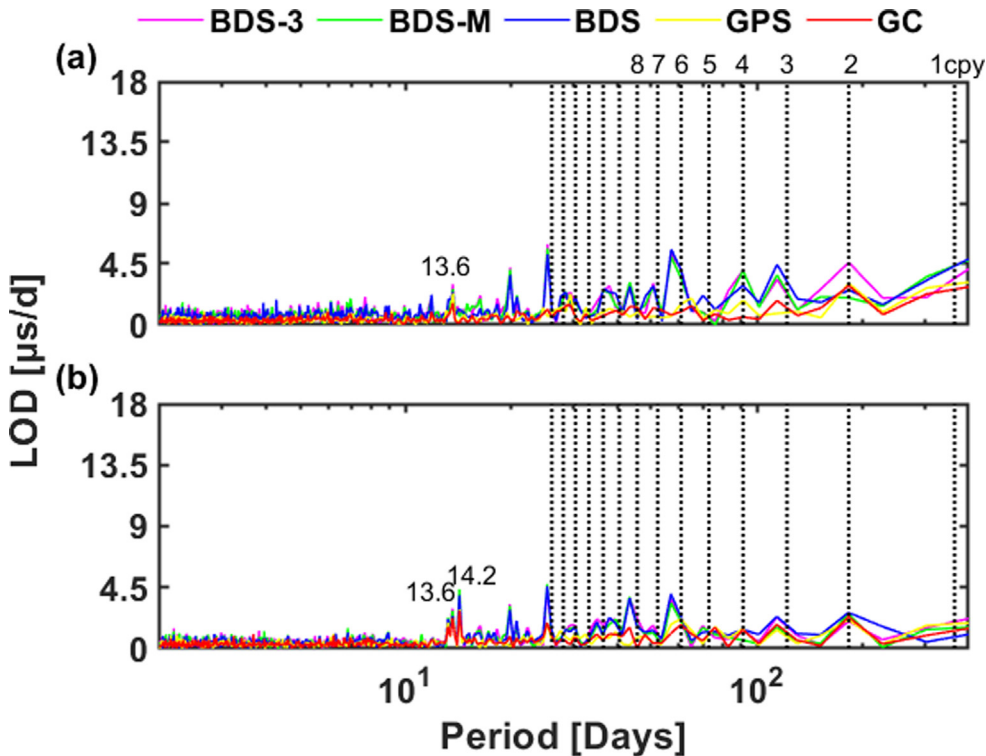


Fig. 11. Amplitude spectra of the estimated LOD residuals with respect to the IERS 14C04 series from 1-day arc solution (top) and 3-day arc solution (bottom). The vertical gray lines denote the harmonics of a draconitic year.

constellation and has little contribution on the decorrelation of LOD and other parameters. With the inclusion of BDS-2 satellites, the STD of BDS solution leads to a

decrease of 5 % compared to BDS-3 results. The STD of the GC combination solution also present a 5 % decrease comparing with GPS solution.

[Fig. 11](#) shows the spectral analysis of the LOD residuals with respect to IERS 14C04 series. From the figures, we can see that BDS-3, BDS-M and BDS solutions show pronounced signals at the period of 2, 3, 4, 6, 14 cpy and the amplitude of the most visible signals is larger than 4.5 $\mu\text{s}/\text{d}$. The switch from 1- to 3-day arc reduce most of these spurious signals and the draconitic year signal at 1 cpy. Moreover, the GC combination can also mitigate these artificial signals. In addition, there is a visible signal occurring in the period of 13.6 days, both for 1 and 3-day arc solution, which originates from the frame alignment with respect to ITRF and the tidal model errors ([Griffiths and Ray, 2013; Ray et al., 2017](#)). Finally, the obvious signal close to 14.2 days occurs in 3-day arc solution, which is introduced by the errors in the conventional model of the sub-daily ERPs and aliasing of the O_1 and M_2 tidal terms ([Griffiths and Ray, 2013; Ray et al., 2017](#)). The signals should at least partly disappear when using the new model of Desai-Sibois with corrected tidal terms ([Desai and Sibois 2016; Sibois 2019](#)).

3.6. ERPs overlaps

The ERPs are modeled as linear between the particular midnight epochs within the orbital arc, assuming a conventional sub-daily motion ([Zajdel et al., 2020](#)). The ERPs derived from 3-day arc have three groups of estimation values at noon epochs for 3 days. Thus, we may calculate the pole coordinates and LOD overlaps between the 3-day arc estimates from the successive days analogously as it is performed for the consecutive orbit arcs in the so-called orbit overlaps ([Lutz et al., 2016](#)). [Table 8](#) shows mean offsets, STD of 3-day arc overlaps for pole coordinates, their rates and LOD. In terms of mean offsets, the absolute values are smaller than 7 μas for X pole coordinates, about 10 μas for Y pole coordinate and smaller than 5 $\mu\text{s}/\text{d}$ for LOD. In terms of STD for pole coordinates, the value of BDS-3, BDS-M and BDS solution is about 80 μas for X component and 90 μas for Y component. The BDS solution makes an improvement of 18 % and 8 % comparing with BDS-3 and BDS-M, respectively. The STD of pole coordinates for GPS and GC solution is about 55 μas and the values for GC solution are about 4 % smaller than GPS solution. As for polar motion rates, the STD of BDS-3 and BDS-M solution is approximately 140 $\mu\text{s}/\text{d}$ for X component and 130 $\mu\text{s}/\text{d}$ for Y component. The STD of BDS pole coordinates has an improvement of about

15 % and 9 % for X and Y component comparing with BDS-3 and BDS-M solutions, respectively. The STD of GC combination solution is about 82 $\mu\text{s}/\text{d}$ and achieves an improvement of about 9 % compared to GPS solution. The STD of LOD is about 8.3 $\mu\text{s}/\text{d}$ for BDS-3, BDS-M and BDS solution while that is approximately 5 $\mu\text{s}/\text{d}$ for GC and GPS solution. The STD of GC combination solution achieves an improvement of about 13 % comparing with GPS solution.

[Fig. 12](#) illustrates the time series of overlaps for the X, Y pole coordinates, their rates and LOD. The figure shows that the overlap residuals are more stable after July/2021 comparing with the time before because more and more GNSS stations support observing BDS-3 satellites. The range of variation in time series is about 300 μas for pole coordinates, 300 $\mu\text{as}/\text{d}$ for pole coordinate rates and 25 $\mu\text{s}/\text{d}$ for LOD. Moreover, the series of overlap residual for GC combination solution are more stable than GPS solution, especially for pole coordinate rates and LOD.

3.7. Geocenter coordinates

As stressed by [Ray et al. \(2017\)](#), the GCC and ERPs should be analyzed simultaneously as GCC solution errors and pole motion errors are correlated in particular for a sub-optimal distribution of GNSS stations. Therefore, the following is the analysis of mean formal errors of GCC estimates and standard deviation of the GCC time series.

The mean formal errors of GCC estimates for particular solutions are presented in [Table 9](#). The mean formal error of 3-day arc is about 1.7 to 2 times better than 1-day arc solution, especially for BDS-3 solution, which is 1.9 to 2 times better than 1-day arc solution in X, Y and Z components. In the case of 3-day arc solution, the mean formal error is about 1.1, 1.1, 1.4 mm for BDS solution and 0.6, 0.6, 0.8 mm for GPS solution, for X, Y and Z component, respectively. The mean formal errors of BDS solution achieve an improvement of about 22 % and 14 % comparing with BDS-3 and BDS-M solutions, respectively.

[Table 10](#) summarizes the mean offsets and STD of the estimated GCC time series. The mean offsets for 3-day arc solution equal 12.4, 10.1, 3.2, 1.9, 0.7 mm for Z component, for BDS-3, BDS-M, BDS, GPS and GC, respectively. The mean offsets of BDS solution is about 4 times better than BDS-3 solution. With the inclusion of IGSO satellites, the mean offsets of BDS solution is about 3.2 times smaller than BDS-M solution. The inclusion of BDS decreases the

Table 8
Statistics for the overlaps of 3-day arc ERPs.

Solutions	X [μas]		Y [μas]		Xrt [$\mu\text{as}/\text{d}$]		Yrt [$\mu\text{as}/\text{d}$]		LOD [$\mu\text{s}/\text{d}$]	
	Mean	STD	Mean	STD	Mean	STD	Mean	STD	Mean	STD
BDS-3	0.8	85.6	8.5	101.3	-39.2	141.1	-1.9	132.8	-3.7	8.5
BDS-M	0.2	77.8	11.6	88.3	-32.9	138.9	-1.5	127.4	-4.0	8.2
BDS	6.5	73.0	9.1	79.6	-31.9	119.1	-9.5	118.7	-3.5	8.2
GPS	-1.2	55.2	9.9	57.2	-20.8	88.4	-9.0	92.7	0.6	5.2
GC	-1.9	53.2	13.9	55.2	-17.0	82.2	-19.7	82.5	-0.8	4.5

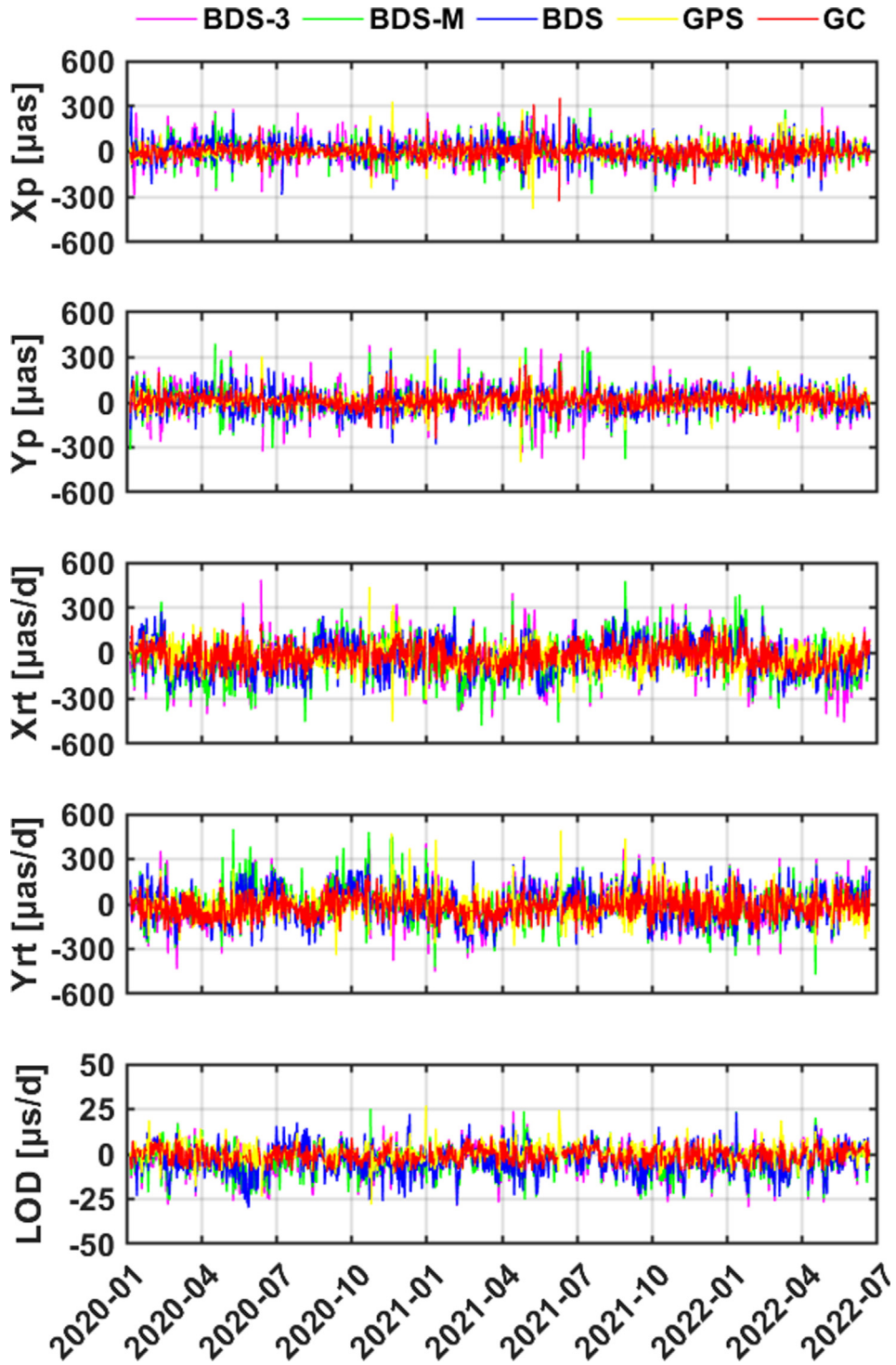


Fig. 12. Overlaps of X and Y pole coordinates and their rates and LOD.

mean offsets by a factor of 2.7 for the GC combination solution than for the GPS solution.

The STD value of GCC for X and Y components is similar and the value for Z component is 1.5 times larger than for X and Y components. The switch from 1 to 3-day arc makes better results. In the case of 3-day arc solution, the STD of GCC, is about 7.2 mm and 8.0 mm for BDS-3 and BDS-M solution, for X and Y components, respec-

tively. This result achieves an improvement of about 27 % and 22 % comparing with 1-day arc solution for X and Y components, respectively. The STD of BDS and GC solutions is about 9.8 mm and 4.2 mm, which makes an improvement of 15 % comparing with 1-day arc solution. The STD in Z component is about 6 mm for GC solution and about 14.4 mm for BDS-3, BDS-M and BDS solution. These results lead to a decrease within 10 % com-

Table 9
Mean formal errors for the respective solutions.

	1-Day arc			3-Day arc		
	X [mm]	Y [mm]	Z [mm]	X [mm]	Y [mm]	Z [mm]
BDS-3	2.6	2.6	3.2	1.4	1.3	1.7
BDS-M	2.3	2.3	2.9	1.3	1.3	1.6
BDS	1.9	2.0	2.6	1.1	1.1	1.4
GPS	1.0	1.0	1.5	0.6	0.6	0.8
GC	1.1	1.1	1.4	0.6	0.6	0.8

Table 10
Mean offsets and standard deviation of the GCC time series for the respective solutions.

	1-Day arc			3-Day arc		
	X	Y	Z	X	Y	Z
Mean offsets (mm)						
BDS-3	2.3	1.9	11.7	1.0	2.1	12.4
BDS-M	0.7	2.6	8.3	0.1	3.2	10.1
BDS	-3.8	17.1	4.0	-5.6	19.3	3.2
GPS	-2.2	5.6	1.1	-1.1	5.6	1.9
GC	-2.8	4.5	0.2	-2.7	6.2	0.7
Standard deviation (mm)						
BDS-3	10.1	10.7	14.9	7.3	8.3	14.7
BDS-M	9.6	9.9	15.0	7.1	7.8	14.2
BDS	10.7	12.1	14.6	9.4	10.2	14.1
GPS	6.0	6.8	10.1	5.6	6.7	9.2
GC	5.9	4.2	7.9	4.8	3.6	6.0

paring with 1-day arc solution. In the 3-day arc case of GPS solution, the STD value is about 5.6, 6.7 and 9.2 mm for X, Y and Z component, which achieves an improvement of 5 % compared to 1-day arc solution. With the inclusion of BDS-2 and IGSO, BDS solution has little improvement for X and Y components and gets an improvement of 5 % for Z component comparing with BDS-3 and BDS-M solution. The STD of GPS solution is about 1.6 times smaller than BDS and the inclusion of BDS gives an improvement of 14 %, 46 % and 35 % for the GC combination solution than GPS, in X, Y and Z components, respectively.

4. Conclusions

The BeiDou system comprises BDS-2 and BDS-3 subsystem and has hybrid constellation, including GEO, IGSO and MEO. In this study, we focus on the estimation of ERPs derived from BDS-3, BDS-M, BDS, GPS as well as the combined GC solutions to study the contribution of BDS-2 and IGSO constellation in BDS solution and the contribution of BDS in GC combination solution. The impacts of the length of the orbital arc from 1-day to 3-day arc, are also discussed in detail. In terms of the quality evaluation, the mean offset and standard deviation of the estimated ERPs with respect to the IERS 14C04 series as well as the spectrum analysis are presented. In addition, we analyze the performance of orbit and GCC, which

are estimated with ERPs simultaneously. The conclusions can be drawn as follows:

- (1) The change of the orbital arc length from 1 to 3 days is beneficial for ERPs quality. The STD of 3-day arc solutions is about 1.4 times better than 1-day arc solutions for X and Y coordinates. In terms of pole coordinate rates, the STD of 3-day arc solution is reduced by 2 to 3.5 times for BDS-3, BDS-M, BDS solutions and 1.5 to 2 times for GPS and GC solutions comparing with 1-day arc solution. As for the STD of LOD, the switching from 1 to 3-day arc length leads to a reduction of 1.3 times for BDS-3, BDS-M, BDS solutions and an improvement of 5 % for GPS and GC solutions.
- (2) Due to the contribution of BDS, the GC combination solution achieves an improvement of 2 %, 2 %, 12 %, 3 % and 5 % comparing with GPS solution for X pole coordinates, Y pole coordinate, X pole coordinate rate, Y pole coordinate rate and LOD, respectively. The STD of 3-day arc solution are 63.3, 62.9 μas for X pole coordinate, 61.7, 57.4 μas for Y pole coordinate, 92.9, 81.3 $\mu\text{as/d}$ for X pole coordinate rates, 88.2, 85.7 $\mu\text{as/d}$ for Y pole coordinate rates and 8.2, 7.8 $\mu\text{s/d}$ for LOD, for GPS and GC solutions, respectively. The mean offsets of the LOD for GPS are visible, which are 2–5 times larger than BDS-based LOD. With the inclusion of BDS, the GC combination can reduce the mean offset by 16 % comparing to GPS solution.
- (3) With the inclusion of BDS-2, the STD for BDS has an improvement of 10 %, 5 %, 5 % for pole coordinate, their rates and LOD when comparing with BDS-3. The inclusion of IGSO can lead to a decrease of about 3 %, 5 % in STD for pole coordinate and their rates for BDS when comparing with BDS-M solution. Finally, the STD of 3-day arc solution are 94.7, 87.9, 86.2 μas for X pole coordinate, 94, 84, 79.9 μas for Y pole coordinate, 126.7, 124.9, 118.9 $\mu\text{as/d}$ for X pole coordinate rates, 117.7, 112.6, 111.5 $\mu\text{as/d}$ for Y pole coordinate rates and 12.5, 11.9, 11.8 $\mu\text{s/d}$ for LOD, for BDS-3, BDS-M, BDS solutions, respectively.
- (4) Since most part of BDS satellites is BDS-3 MEO constellation, which is similar with Galileo and GNSS constellation with 3 orbital planes, the BDS-3, BDS-M and BDS solutions are suffered from 3 cpy spurious signals, but the amplitude for BDS is lower than that for BDS-3 and BDS-M. The visible signal close to 7 cpy (52 days) in polar motion arising in BDS-3, BDS-M and BDS, which may be caused by the deficiencies of orbital modeling. The pronounced spurious signal at the period of 7 days in pole coordinate and its rates estimates for BDS-3 and BDS-M can be reduced by BDS solution. The visible spurious signals at 13.6 days and 14.2 days in LOD are lower for BDS than for BDS-3 and BDS-M. The GC com-

bination solution and the extension of arc length can mitigate these artificial signals and draconitic signals. Moreover, with the inclusion of BDS, the GC solution has lower spurious signals and draconitic signals than GPS solution, especially for LOD at 1, 2, 6 cpy.

Since the ERPs are susceptible to absorbing the spurious effects from orbit modeling deficiencies, especially the deficiencies in the solar radiation pressure, the combination of box-wing model with ECOM series model has been investigated to be able to improve the quality of orbit and geodetic parameters for BDS (Duan et al., 2022; Li et al., 2022; Peng et al., 2022). Therefore, we aim to add the box-wing model as a priori model in the next step, which may enhance our results. To further improve the quality of ERPs derived from BDS, more homogeneous BDS stations and accurate PCV values should be gave to reach the same quality level of ERPs from GPS.

Declaration of Competing Interest

The authors declare that they have no known competing financial interests or personal relationships that could have appeared to influence the work reported in this paper.

Acknowledgements

The authors acknowledge the IGS MGEX, ESA and IERS for providing the Multi-GNSS data, ESA Multi-GNSS products and ERPs products. The numerical computations in the study are performed using the supercomputing system in the Supercomputing Center of Shandong University at Weihai. This study is supported by the National Natural Science Foundation of China (41874032 and 42204015); State Key Laboratory of Geodesy and Earth's Dynamics, Innovation Academy for Precision Measurement Science and Technology, Chinese Academy of Sciences (SKLGED2021-3-4). We would like to thank Editor-in-Chief and three anonymous reviewers for their constructive comments and suggestions. Finally, we want to express our special thanks to Prof. Markus Rothacher and Prof. Rolf Dach for their helpful discussions with us in the data processing.

References

- Arnold, D., Meindl, M., Beutler, G., Dach, R., Schaer, S., Lutz, S., Prange, L., Sosnica, K., Mervart, L., Jaggi, A., 2015. CODE's new solar radiation pressure model for GNSS orbit determination. *J. Geod.* 89, 775–791. <https://doi.org/10.1007/s00190-015-0814-4>.
- Beutler, G., Brockmann, E., Gurtner, W., Hugentobler, U., Mervart, L., Rothacher, M., Verdun, A., 1994. Extended orbit modeling techniques at the CODE processing center of the international GPS service for geodynamics (IGS): theory and initial results. *Manuscr Geodaet* 19, 367–386.
- Bizouard, C., Lambert, S., Gattano, C., Becker, O., Richard, J.Y., 2019. The IERS EOP 14C04 solution for Earth orientation parameters consistent with ITRF 2014. *J. Geod.* 93, 621–633. <https://doi.org/10.1007/s00190-018-1186-3>.
- Boehm, J., Niell, A., Tregoning, P., Schuh, H., 2006. Global Mapping Function (GMF): A new empirical mapping function based on numerical weather model data. *Geophys. Res. Lett.* 33. <https://doi.org/10.1029/2005gl025546>.
- Chen, G., Herring, T.A., 1997. Effects of atmospheric azimuthal asymmetry on the analysis of space geodetic data. *J. Geophys. Res.-Solid Earth* 102, 20489–20502. <https://doi.org/10.1029/97jb01739>.
- Dach, R., Brockmann, E., Schaer, S., Beutler, G., Meindl, M., Prange, L., Bock, H., Jaggi, A., Ostini, L., 2009. GNSS processing at CODE: status report. *J. Geod.* 83, 353–365. <https://doi.org/10.1007/s00190-008-0281-2>.
- Dach, R., Lutz, S., Walser, P., Fridez, P. (Eds.), 2015. Bernese GNSS Software Version 5.2. User manual, Astronomical Institute, University of Bern, Bern Open Publishing. <http://doi.org/10.7892/boris.72297>; ISBN: 978-3-906813-05-9.
- Dach, R., Selmke, I., Villiger, A., Arnold, D., Prange, L., Schaer, S., Sidorov, D., Stebler, P., Jaggi, A., Hugentobler, U., 2021. Review of recent GNSS modelling improvements based on CODEs Repro3 contribution. *Adv. Space Res.* 68, 1263–1280. <https://doi.org/10.1016/j.asr.2021.04.046>.
- Desai, S.D., Sibois, A.E., 2016. Evaluating predicted diurnal and semidiurnal tidal variations in polar motion with GPS-based observations. *J. Geophys. Res. Solid Earth* 121, 5237–5256. <https://doi.org/10.1002/2016JB013125>.
- Dow, J.M., Neilan, R.E., Rizos, C., 2009. The International GNSS Service in a changing landscape of Global Navigation Satellite Systems. *J. Geod.* 83, 191–198. <https://doi.org/10.1007/s00190-008-0300-3>.
- Duan, B., Hugentobler, U., Selmke, I., Marz, S., Killian, M., Rott, M., 2022. BeiDou satellite radiation force models for precise orbit determination and geodetic applications. *IEEE Trans. Aerosp. Electron. Syst.* 58, 2823–2836. <https://doi.org/10.1109/TAES.2021.3140018>.
- Ferland, R., Piraszewski, M., 2009. The IGS-combined station coordinates, Earth rotation parameters and apparent geocenter. *J. Geod.* 83, 385–392. <https://doi.org/10.1007/s00190-008-0295-9>.
- Griffiths, J., Ray, J.R., 2013. Sub-daily alias and draconitic errors in the IGS orbits. *GPS Solutions* 17, 413–422. <https://doi.org/10.1007/s10291-012-0289-1>.
- Kouba, J., Mireault, Y., 1998. New IGS ERP Format (version 2). <https://files.igs.org/pub/data/format/erp.txt>. Last access: 25 Nov. 2022.
- Li, X., Huang, S., Yuan, Y., Zhang, K., Lou, J., 2022. Geocenter motions derived from BDS observations: Effects of the solar radiation pressure model and constellation configuration. *GPS Solutions*, <https://doi.org/10.21203/rs.3.rs-1949256/v1>.
- Lutz, S., Schaer, S., Dach, R., Beutler, G., Steigenberger, P., Meindl, M., Jaggi, A., 2014. Earth rotation and GNSS orbits from one-day and three-day arcs. In: EGU General Assembly Conference Abstracts. <https://meetingorganizer.copernicus.org/EGU2014/EGU2014-12212.pdf>.
- Lutz, S., Meindl, M., Steigenberger, P., Beutler, G., Sosnica, K., Schaer, S., Dach, R., Arnold, D., Thaller, D., Jaggi, A., 2016. Impact of the arc length on GNSS analysis results. *J. Geod.* 90, 365–378. <https://doi.org/10.1007/s00190-015-0878-1>.
- Lyard, F., Lefevre, F., Letellier, T., Francis, O., 2006. Modelling the global ocean tides: modern insights from FES2004. *Ocean Dyn.* 56, 394–415. <https://doi.org/10.1007/s10236-006-0086-x>.
- Mayer V., Springer T., Schonemann E., Enderle W. (2019). ESA Multi-GNSS Products. Presentation, EGU General Assembly 2019, April 07–12, Vienna, Austria. http://navigation-office.esa.int/attachments_48824764_1_EsaMgnss_EGU2019_VolkerMayer_final.pdf.
- Meindl, M., 2011. Combined analysis of observations from different global navigation satellite systems. University of Bern, Bern: Geodätisch-geophysikalische Arbeiten in der Schweiz, vol 83, Schweizerische Geodätische Kommission.
- MGEX, 2020. BDS Constellations. <https://mgex.igs.org/mgex/constellations/#beidou>. Last accessed 1st November 2021

- Mireault, Y., Kouba, J., Ray, J., 1999. IGS Earth Rotation Parameters. *GPS Solutions* 3, 59–72. <https://doi.org/10.1007/pl00012781>.
- Montenbruck, O., Steigenberger, P., Prange, L., Deng, Z., Zhao, Q., Perosanz, F., Romero, I., Noll, C., Stürze, A., Weber, G., Schmid, R., MacLeod, K., Schaer, S., 2017. The Multi-GNSS Experiment (MGEX) of the International GNSS Service (IGS) – Achievements, prospects and challenges. *Adv. Space Res.* 59, 1671–1697. <https://doi.org/10.1016/j.asr.2017.01.011>.
- Pavlis, N.K., Holmes, S.A., Kenyon, S.C., Factor, J.K., 2012. The development and evaluation of the Earth Gravitational Model 2008 (EGM2008). *J. Geophys. Res.-Solid Earth* 117. <https://doi.org/10.1029/2011jb008916>.
- Peng, Y., Lou, Y., Dai, X., Guo, J., Shi, C., 2022. Impact of solar radiation pressure models on Earth rotation parameters derived from BDS. *GPS Solutions* 26, 126. <https://doi.org/10.1007/s10291-022-01316-1>.
- Petit, G., Luzum, B., 2010. IERS Technical Note No. 36, IERS Conventions (2010). In: International Earth Rotation and Reference Systems Service. <https://www.iers.org/IERS/EN/Publications/TechnicalNotes/tn36.html>.
- Prange, L., Orliac, E., Dach, R., Arnold, D., Beutler, G., Schaer, S., Jaggi, A., 2017. CODE's five-system orbit and clock solution—the challenges of multi-GNSS data analysis. *J. Geod.* 91, 345–360. <https://doi.org/10.1007/s00190-016-0968-8>.
- Prange, L., Beutler, G., Dach, R., Arnold, D., Schaer, S., Jaggi, A., 2020. An empirical solar radiation pressure model for satellites moving in the orbit-normal mode. *Adv. Space Res.* 65, 235–250. <https://doi.org/10.1016/j.asr.2019.07.031>.
- Ray, J., Rebischung, P., Griffiths, J., 2017. IGS polar motion measurement accuracy. *Geod. Geodyn.* 8, 413–420. <https://doi.org/10.1016/j.geog.2017.01.008>.
- Rebischung, P., Altamimi, Z., Ray, J., Garayt, B., 2016a. The IGS contribution to ITRF2014. *J. Geod.* 90, 611–630. <https://doi.org/10.1007/s00190-016-0897-6>.
- Rebischung, P., Schmid, R., 2016b. IGS14/igs14.atx: a new framework for the IGS Products. In: American geophysical union fall meeting 2016 San Francisco, USA. https://media.tum.de/doc/13413_38/file.pdf.
- Rodriguez-Solano, C.J., Hugentobler, U., Steigenberger, P., Blossfeld, M., Fritsche, M., 2014. Reducing the draconitic errors in GNSS geodetic products. *J. Geod.* 88, 559–574. <https://doi.org/10.1007/s00190-014-0704-1>.
- Rothacher, M., Beutler, G., Herring, T.A., Weber, R., 1999. Estimation of nutation using the Global Positioning System. *J. Geophys. Res. Solid Earth* 104, 4835. <https://doi.org/10.1029/1998jb900078>.
- Rothacher, M., Beutler, G., Weber, R., Hefty, J., 2001. High-frequency variations in Earth rotation from Global Positioning System data. *J. Geophys. Res.-Solid Earth* 106, 13711–13738. <https://doi.org/10.1029/2000jb900393>.
- Scaramuzza, S., Dach, R., Beutler, G., Arnold, D., Susnik, A., Jaggi, A., 2018. Dependency of geodynamic parameters on the GNSS constellation. *J. Geod.* 92, 93–104. <https://doi.org/10.1007/s00190-017-1047-5>.
- Sibois, A., 2019. Analysis of high frequency EOP (HFEOP) models and their impact on GPS data processing. In: International GNSS Service: Analysis Centre Workshop 2019, 15–17 April, Potsdam, Germany. URL: https://s3-ap-southeast-2.amazonaws.com/igs-acc-web/igs-acc-website/workshop2019/Sibois_IgsAcWorkshop_2019.pdf. Last accessed 20th November 2022.
- Standish, E., 1998. *JPL planetary and lunar ephemerides, DE405/LE405. JPL IOM 312, F-98_048*.
- Steigenberger, P., Rothacher, M., Dietrich, R., Fritsche, M., Rulke, A., Vey, S., 2006. Reprocessing of a global GPS network. *J. Geophys. Res.-Solid Earth* 111. <https://doi.org/10.1029/2005jb003747>.
- Zajdel, R., Sosnica, K., Bury, G., Dach, R., Prange, L., 2020. System-specific systematic errors in Earth rotation parameters derived from GPS, GLONASS, and Galileo. *GPS Solutions* 24. <https://doi.org/10.1007/s10291-020-00989-w>.